3D Dynamical Modeling of the Gamma-ray Binary LS 5039

Atsuo T. Okazaki
(Hokkai-Gakuen Univ.),
Christopher M.P. Russell
(Hokkai-Gakuen Univ.)
and
Stanley P. Owocki
(Univ. of Delaware, USA)

Outline

- Introduction to the VHE gamma-ray binaries
- LS 5039: Previous results
- LS 5039: 3D SPH simulations
- Concluding remarks

Introduction to the VHE Gamma-ray Binaries

VHE gamma-ray binaries (1)

- Only 5 systems, all of which consist of an OB star and a compact object.
  - **3 systems with a Be star**
  - **2 systems with a main-seq. O star**
- Nature of the compact object established only for one system (PSR B1259-63).
- Two competing scenarios for other systems: **Pulsar wind (PW) scenario vs. Microquasar (MQ) scenario**

Be Stars

Hydrogen spectrum

Non-supergiant B stars with emission lines

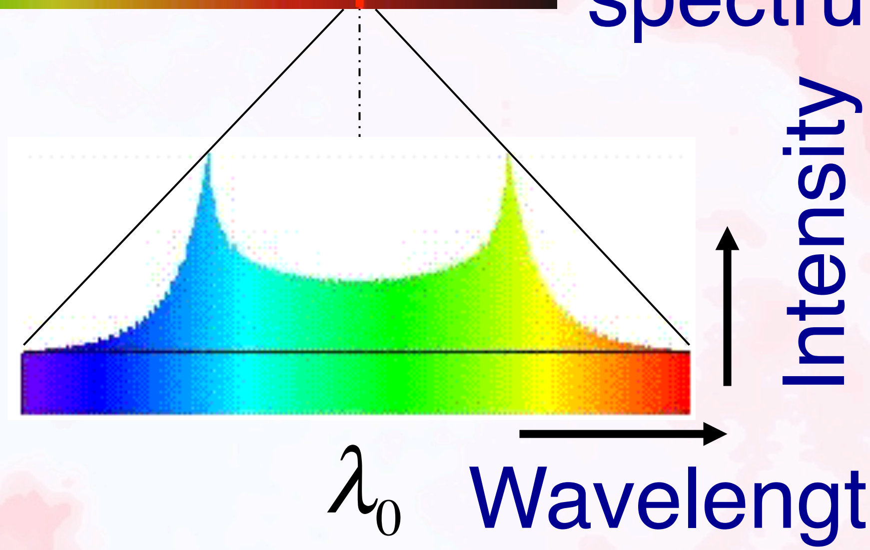

Viscous decretion disk

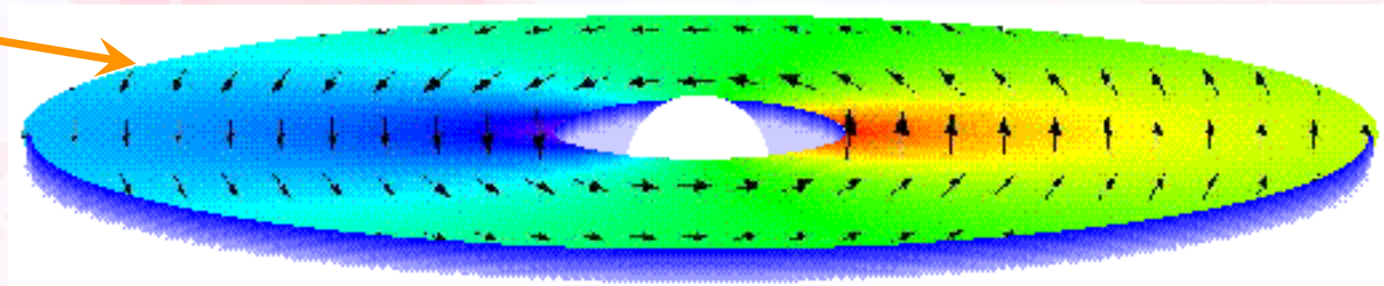

Courtesy of Stan Owocki

VHE gamma-ray binaries (2)

System	Scenario	Optical star	P_{orb} (d)	e
PSR B1259-63	PW	Be	1237	0.87
LS I +61 303	MQ(?)	Be	26.5	0.54
HESS J0632+057	?	Be	321 (315)	0.83
LS 5039	PW(?)	O	3.9	0.35
1FGL J1018.6-5856	?	O	16.6	low

Our motivations

- Why do only massive binaries show VHE gamma-rays?
- Does the PW scenario work for all VHE gamma-ray binaries? Or, does the MQ scenario work for some systems?
- In systems with Be stars, what’s the role of the Be disk for high energy emission?

Study of VHE gamma-ray binaries

3D dynamical modeling helps

Is a new frontie … **research**. The cur… goals are:

- to understand the nature of individual systems, including
  - physics of interactions
  - origin of high energy emission
- to establish a classification/ unification scheme of these systems

Shape of the colliding-wind interaction front without orbital motion

Momentum balance determines the bow shock structure (e.g., Canto et al. 1996)

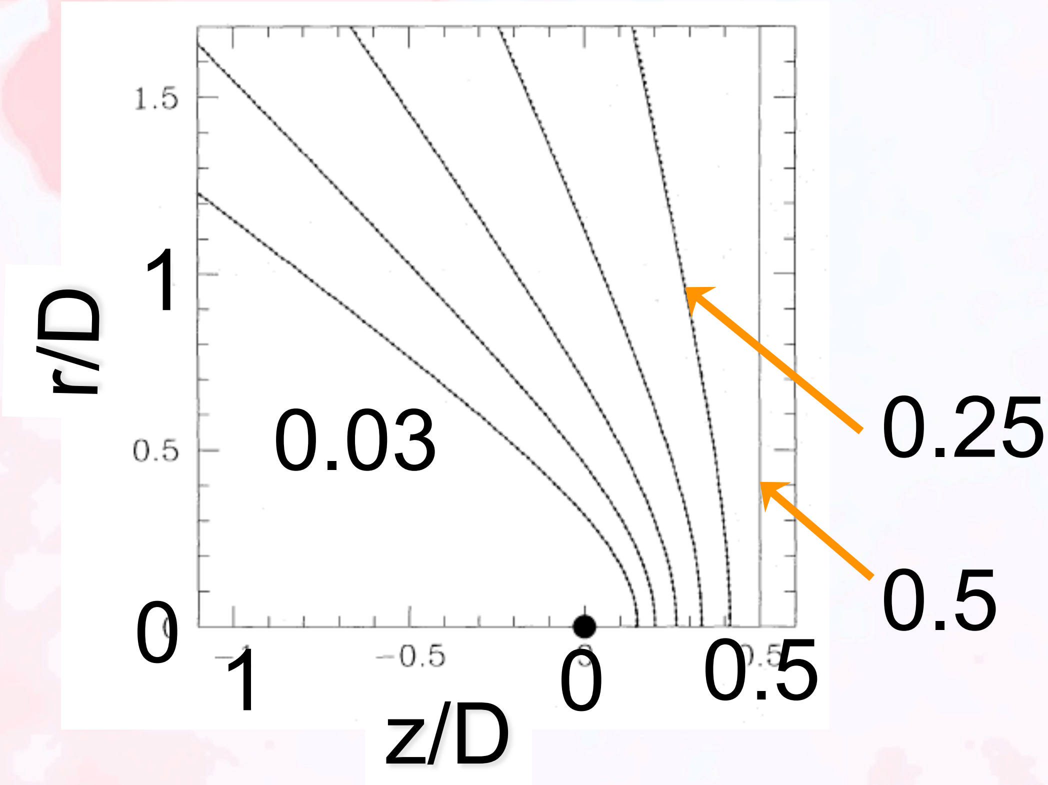

$$\eta \equiv \frac{\dot{M}_2 v_2}{\dot{M}_1 v_1}$$

Interaction in a Be-star system (1)

PSR B1259-63 — radio pulsar

LS 2883 — O9.5e

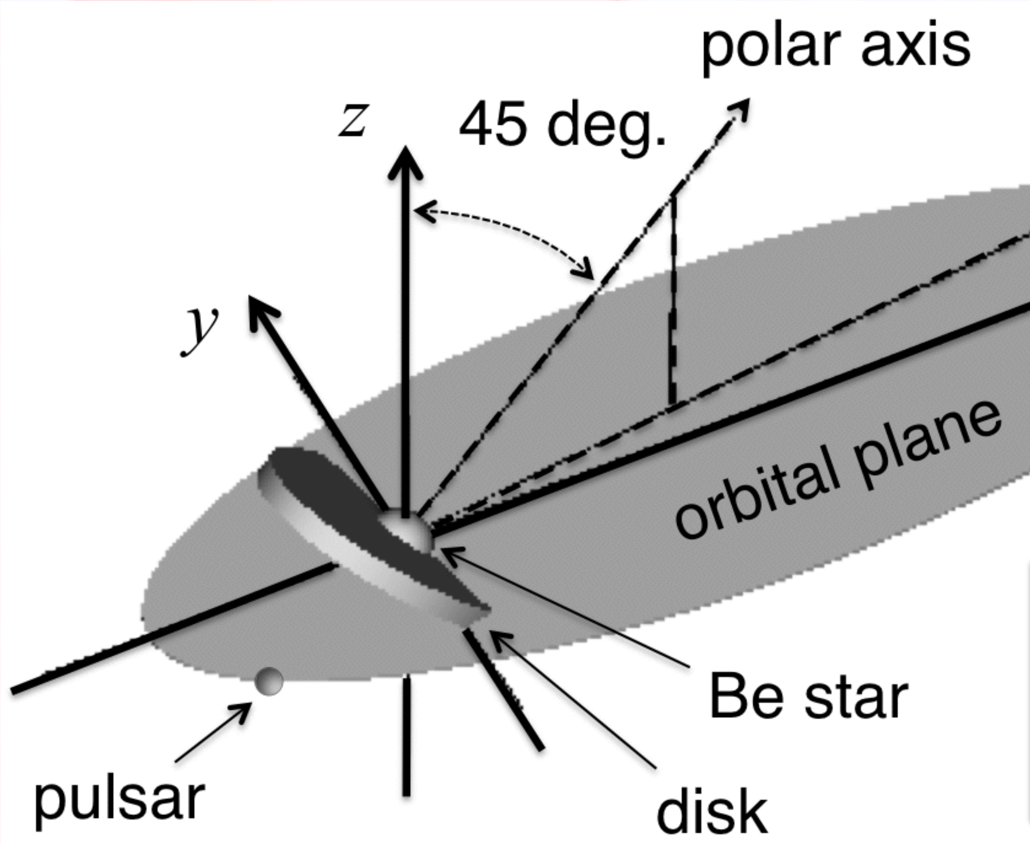

$P_{\mathrm{orb}} \sim 3.4\,\mathrm{yr}$,
$e = 0.87$

Interaction in a Be-star system: an example

Widely-accepted picture of the PW-Be disk interaction in PSR B1259-63 ➡ **Is this realistic?**

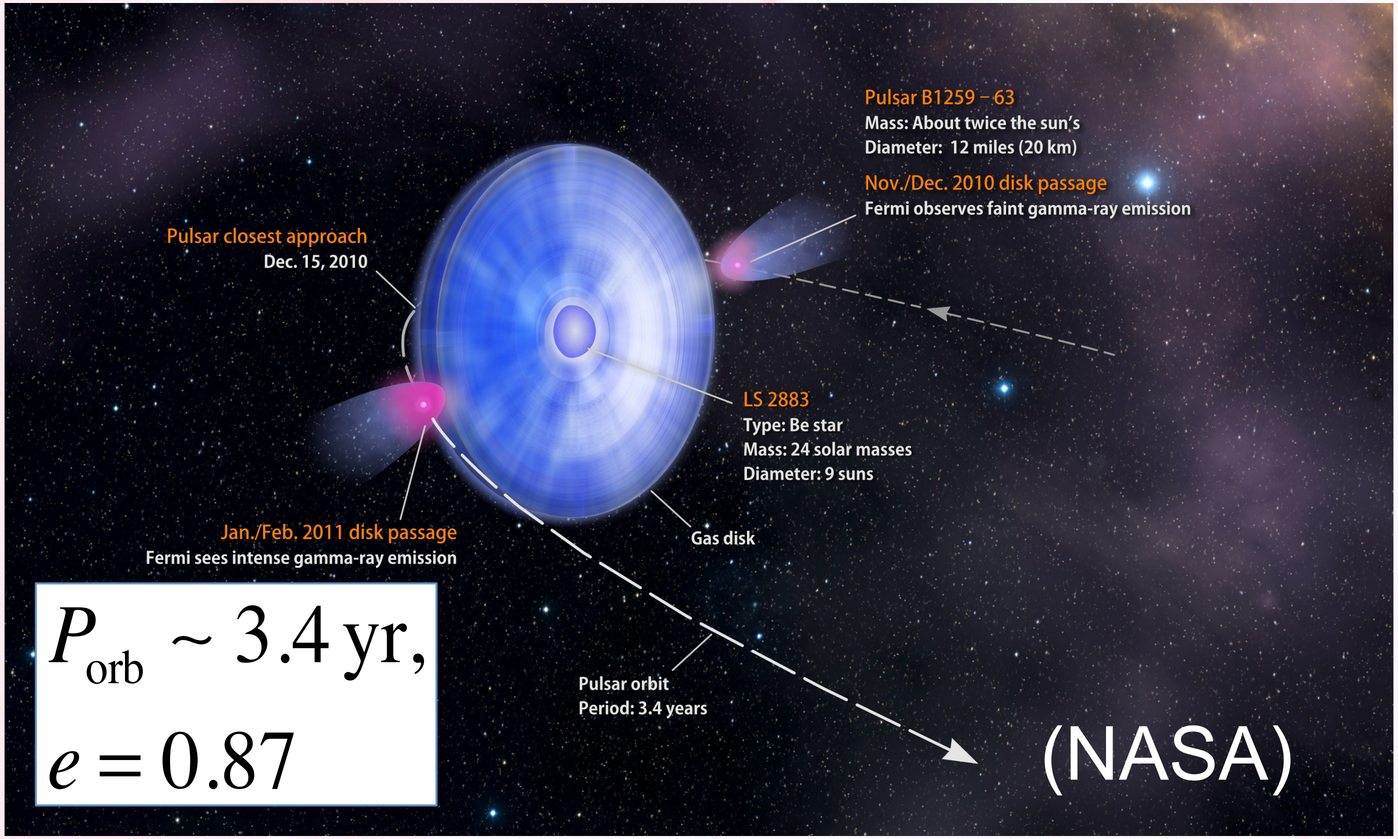

PW-Be star interaction is much more complicated

$\rho_0 = 10^{-9}$ g cm^{-3}

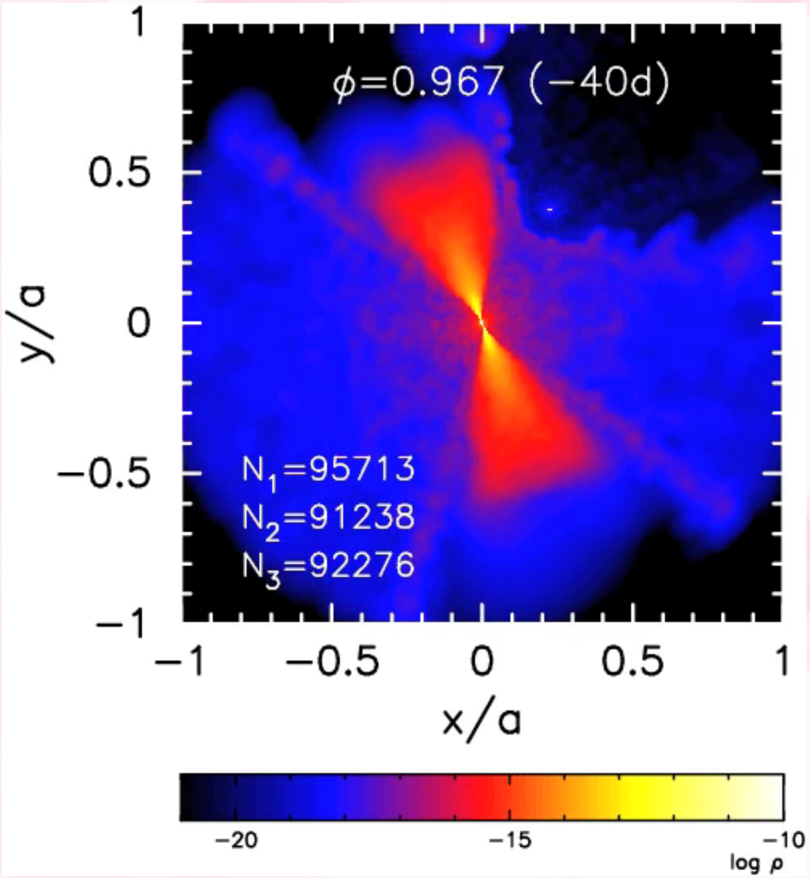

Density on orbital plane

Pulsar passes through Be disk

→ termination of PW over a large solid angle

→ Efficient conversion of PW power to non-thermal emission

(Takata+ 2012)

Structure of shocked winds is time-dependent and 3D! (Takata+ 2012)

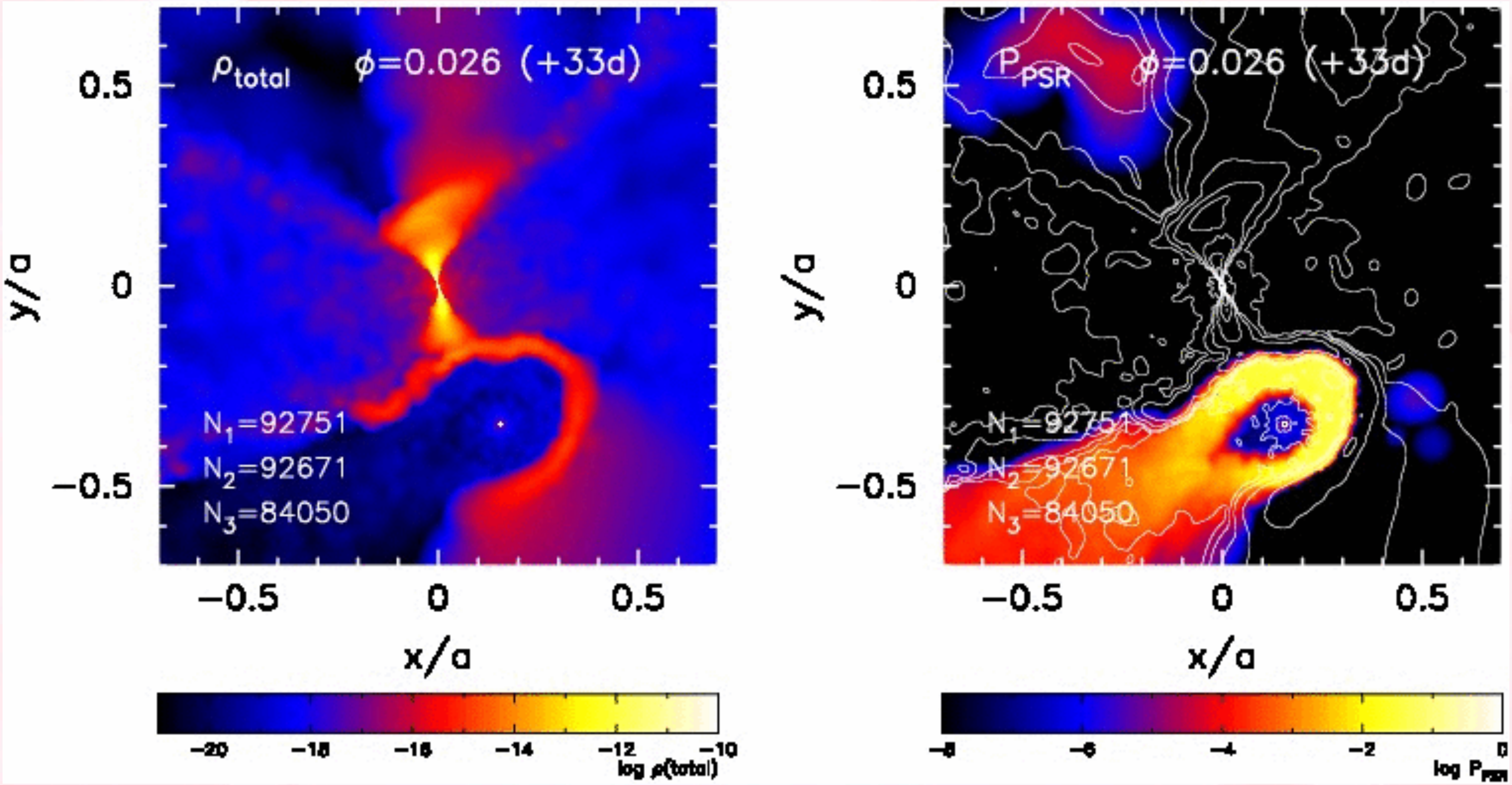

Density on orbital plane

PW pressure on orbital plane

High energy emission from the shocked pulsar wind (2) (Takata+ 2012)

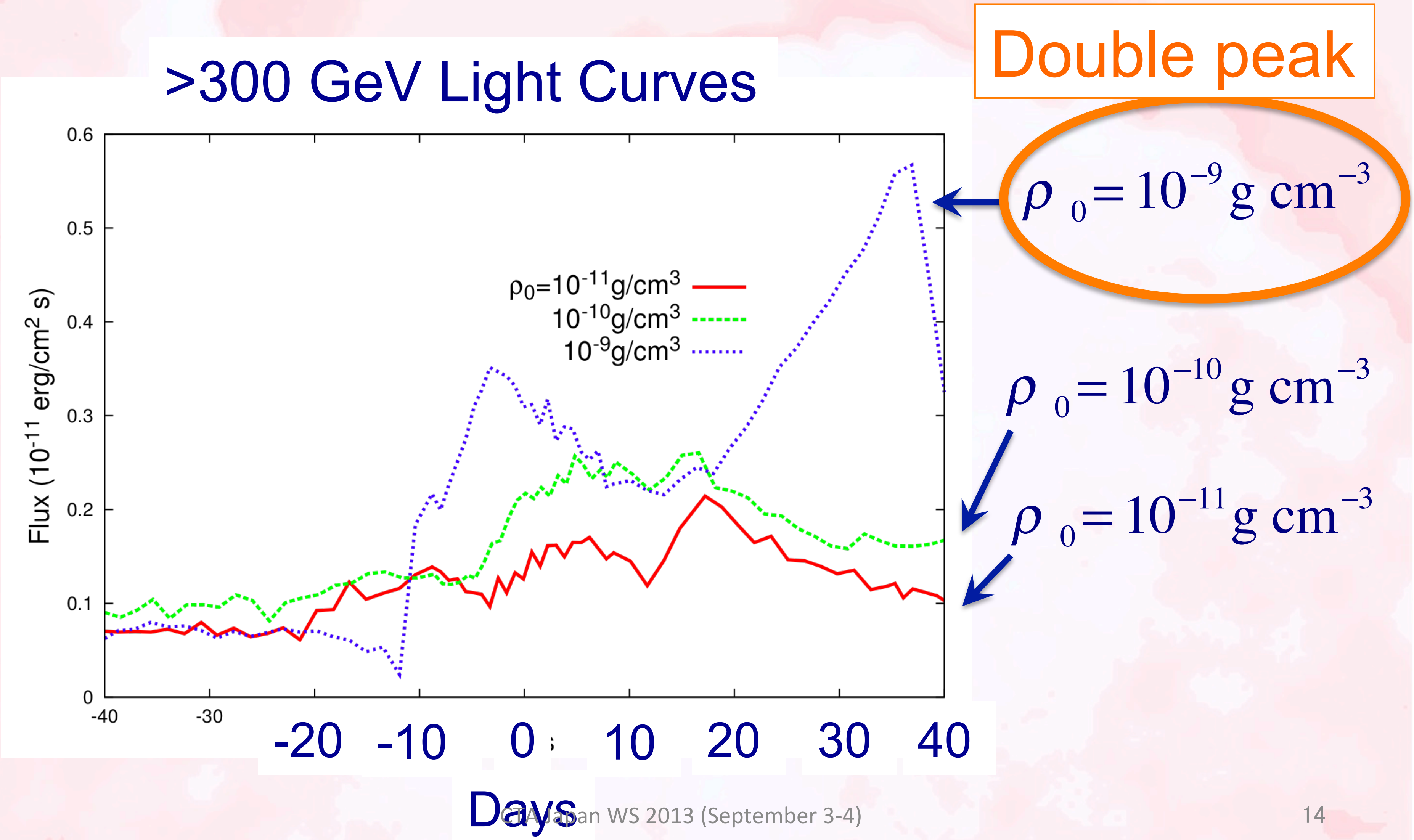

LS 5039: Previous results

Observed features

O6.5V + compact object: P_{orb}=3.906d, e=0.35

(Casares 2013)

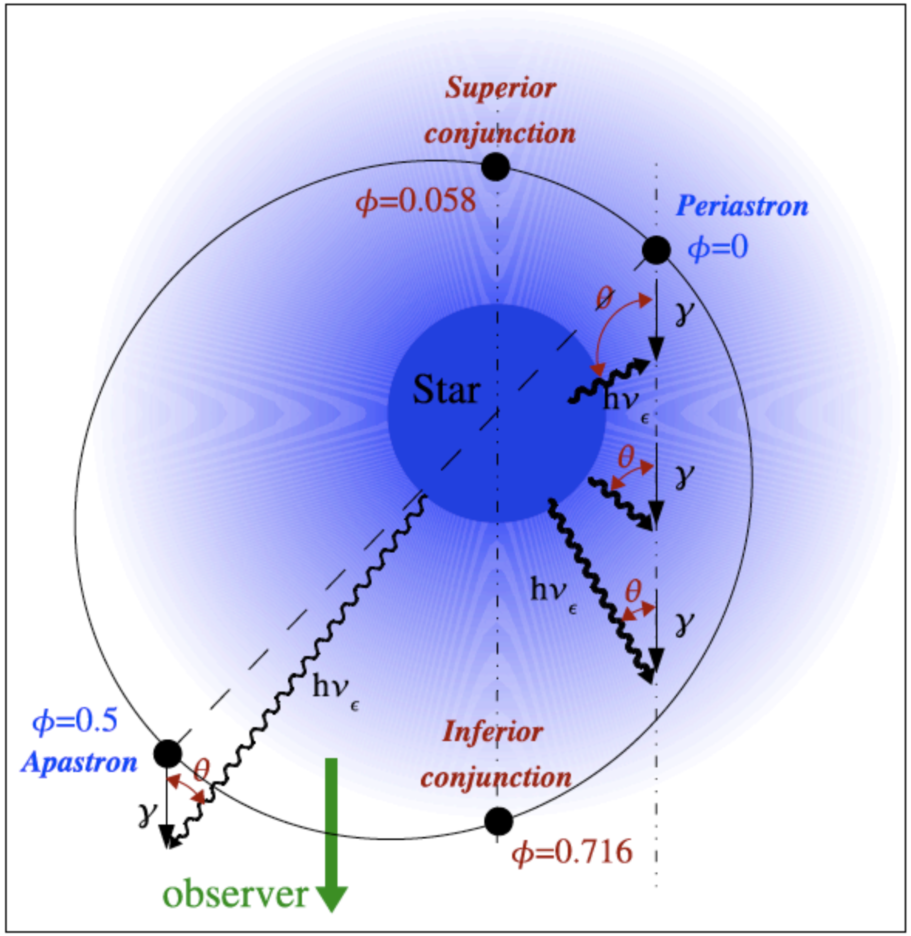

(Aharonian et al. 2006)

Fermi & HESS Observations

- **Fermi 0.1-10 GeV peaks near sup. conj.** (Abdo et al. 2006)
- **HESS 1-40 TeV peaks near inf. conj.** (Aharonian et al. 2006)
- **X-ray lightcurve similar to that in TeV** (Takahashi et al. 2009)

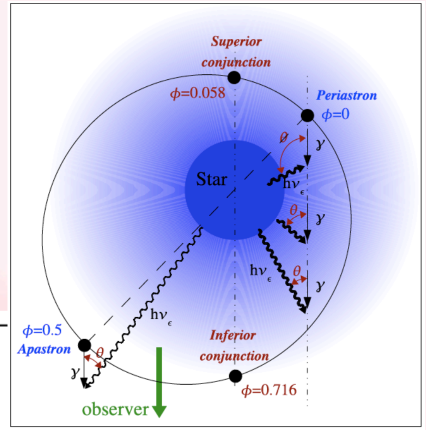

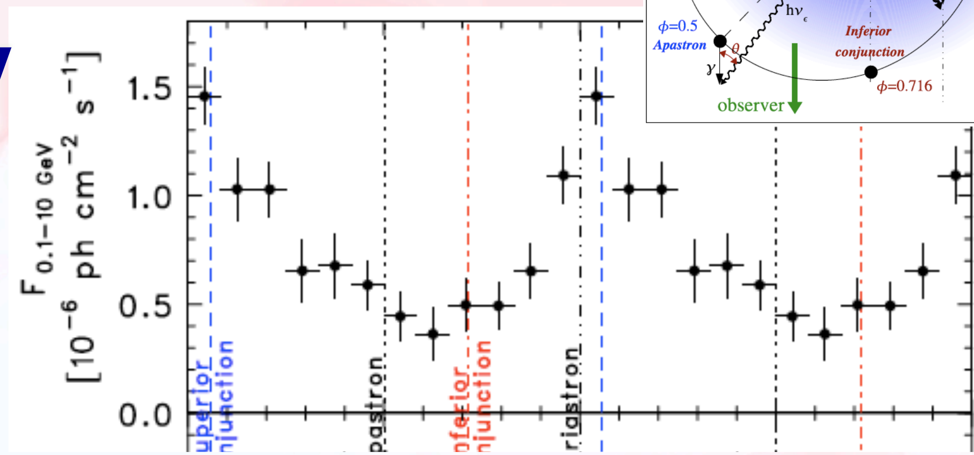

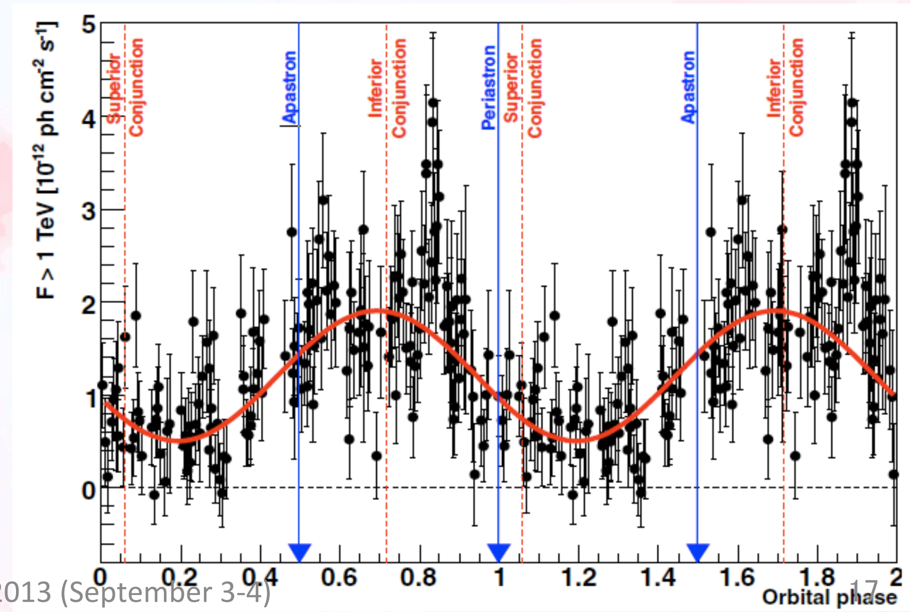

Observed features that favor PW scenario
(Marc Ribo@Variable Galactic Gamma-ray Sources)

- VLBA map regularly varies with orbital phase, and is compatible with PW scenario.
- All emission in radio, X-rays, GeV gamma-rays, and TeV gamma-rays behave similarly. No MQs do that.
- LS 5039 shows no state change. MQs show jets at some particular states.

VLBI map + a simple model
➡ inclination angle 60-75 deg.

(Moldon et al. 2012)

Emitting region adopted by Moldon et al. (2012)

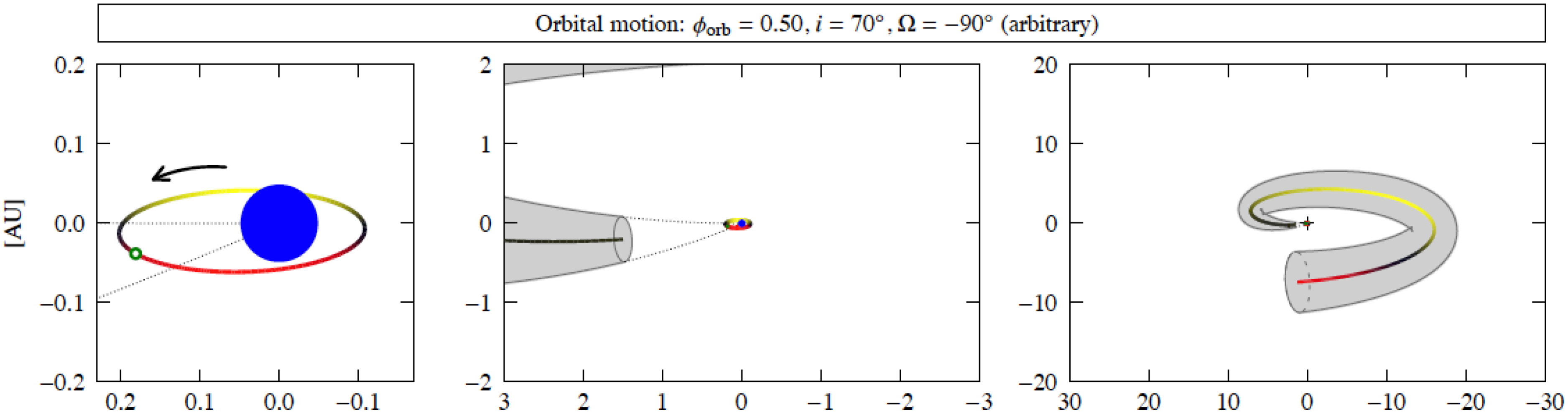

But, the PW cone can't be this thin.

HE/VHE Gamma-ray emission calculation via relativistic 2D simulations

Zabalza et al. (2012)

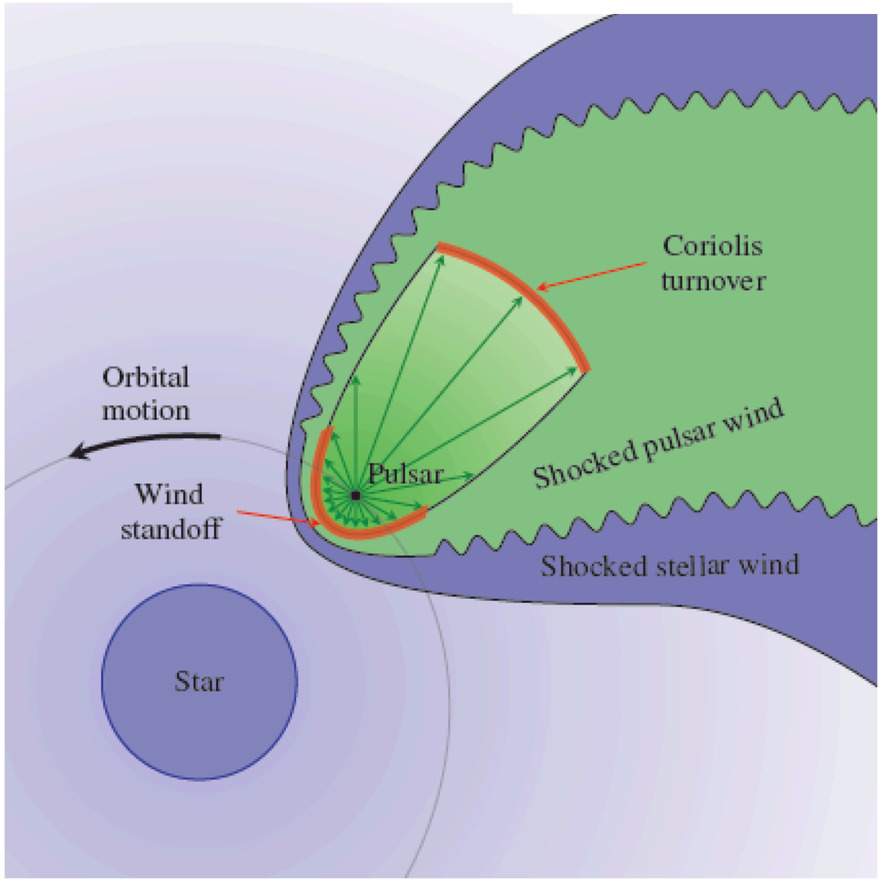

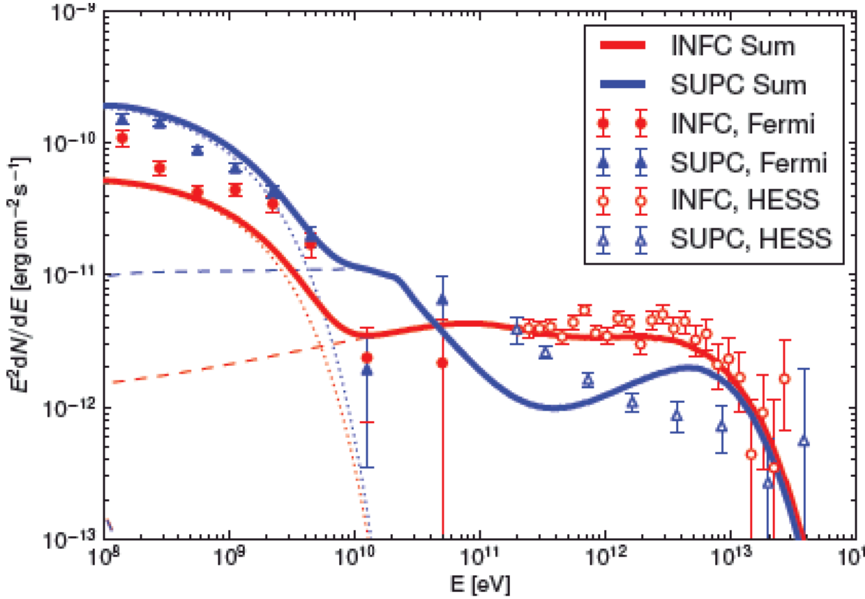

Fig. 2. Spectral energy distribution of LS 5039. The computed emission and observational data during the inferior conjunction ($0.45 < \phi < 0.9$) is shown in red and during the superior conjunction ($0.9 < \phi < 0.45$) in blue. The emission components from the wind standoff and Coriolis turnover locations are indicated with a dotted and dashed line, respectively.

Thermal X-ray flux/spectrum

- So far, no significant thermal X-rays have been detected for any VHE binaries.
- The upper limit of EW(Fe line) is 40eV (Takahashi et al. 2009)
- But, thermal X-rays could be detected by future missions, such as ASTRO-H.
- Even if it is too weak to be detected, it can be used to constrain the spin down luminosity of the pulsar (Zabalza et al. 2011).

Semi-analytical shock structuere model by Zabalza et al. (2011)

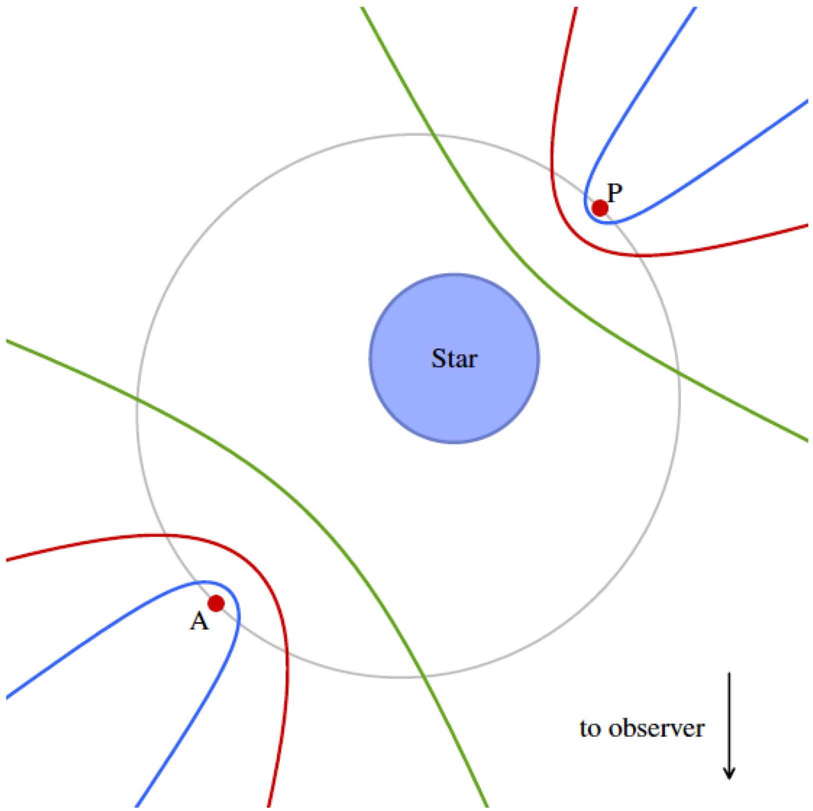

Figure 2. Sketch of the orbit of the compact object around the companion star in LS 5039. The star (but not the pulsar) is to scale. The two marked positions correspond to periastron (P) and apastron (A). For each of these positions the shape of the CD is shown for $\eta_\infty = 0.0025, 0.025,$ and 0.25 (blue, red, and green lines, respectively).

$$L_{sd} = 3\times10^{35}\,\mathrm{erg/s}$$

$$L_{sd} = 3\times10^{36}\,\mathrm{erg/s}$$

$$L_{sd} = 3\times10^{37}\,\mathrm{erg/s}$$

Thermal X-ray spectra
(Zabalza et al. 2011)

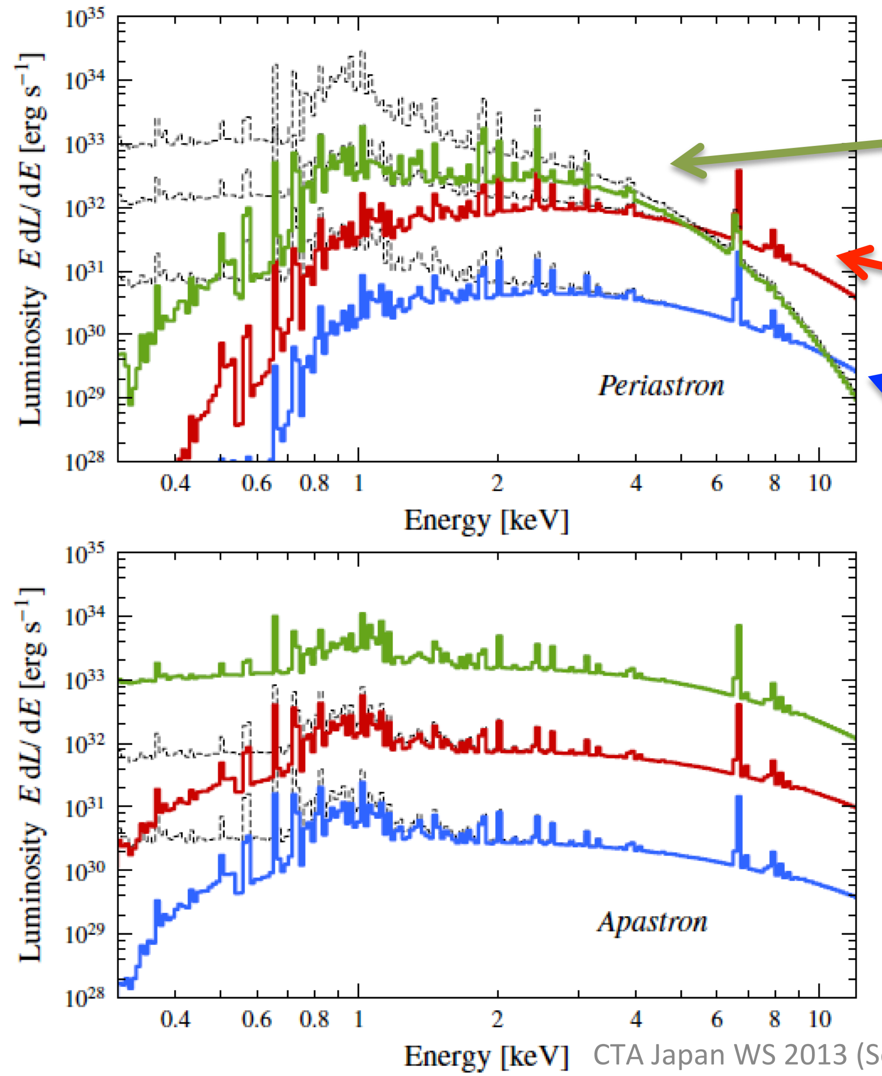

$L_{sd} = 3\times10^{37}$ erg/s

$L_{sd} = 3\times10^{36}$ erg/s

$L_{sd} = 3\times10^{35}$ erg/s

Upper limit of pulsar spin down luminosity
(Zabalza et al. 2011)

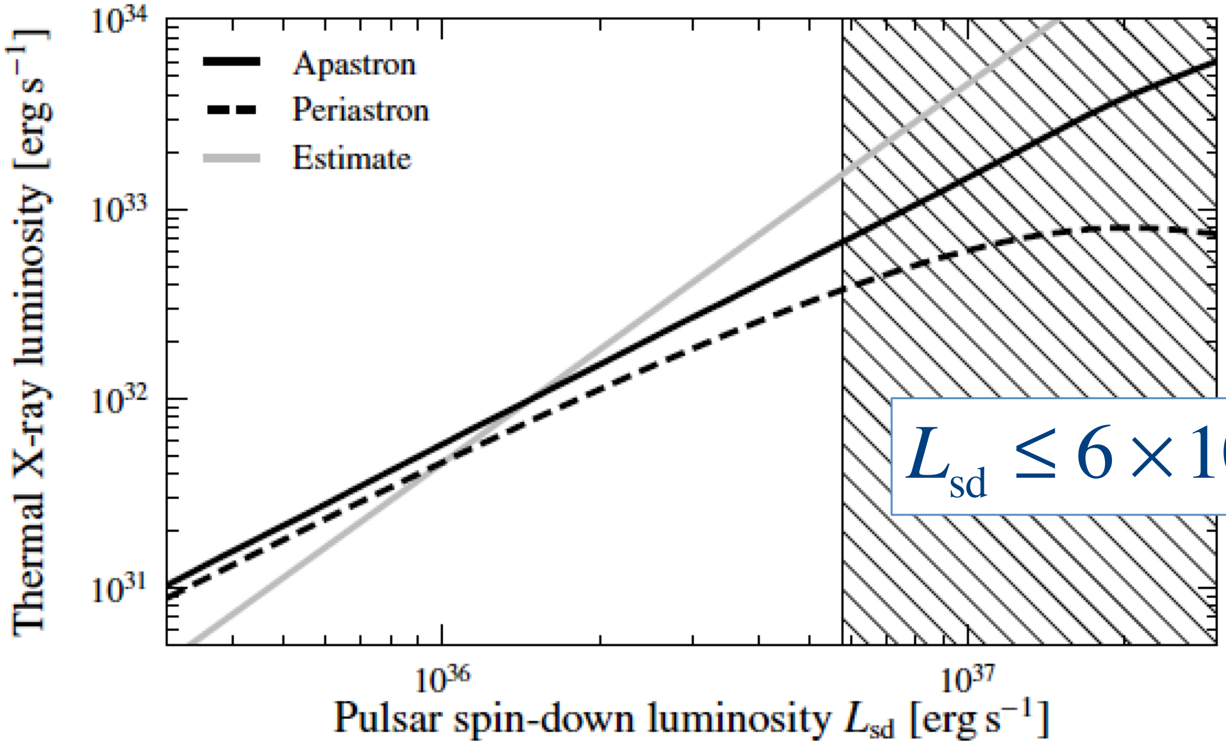

$$L_{sd} \leq 6 \times 10^{36}\,\mathrm{erg/s}$$

Figure 3. Thermal emission luminosity in the 0.3–10 keV range as a function of the spin-down luminosity of the pulsar. The fluxes at periastron (solid) and apastron (dashed) are shown. In addition, the rough estimate of Equation (4) is shown as a gray line. The range of pulsar spin-down luminosities excluded by the thermal emission is shown as a hatched region. In all cases, a mass-loss rate of $2.65 \times 10^{-7}\ M_{\odot}\ \mathrm{yr}^{-1}$ was assumed.

LS 5039: 3D SPH simulations

Numerical method: Hydro simulations

- 3D Smoothed Particle Hydrodynamics code
- Stellar wind: $v_{\mathrm{w}} = v_{\infty}(1 - R / r)^{\beta}$ with $\beta = 1$
- **Pulsar wind: relativistic pulsar wind modeled by a high-velocity, non-relativistic wind with the same momentum flux**
- Optically-thin radiative cooling

SPH (Smoothed Particle Hydrodynamics)

A particle method that divides fluid into a set of discrete "fluid elements” (=particles).

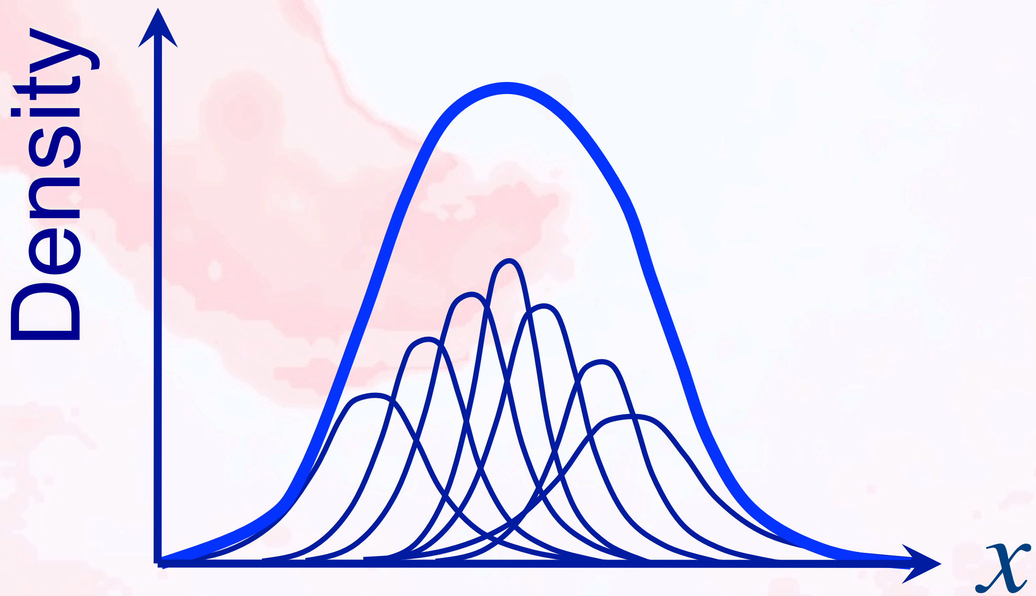

Numerical method: radiative transfer

observer

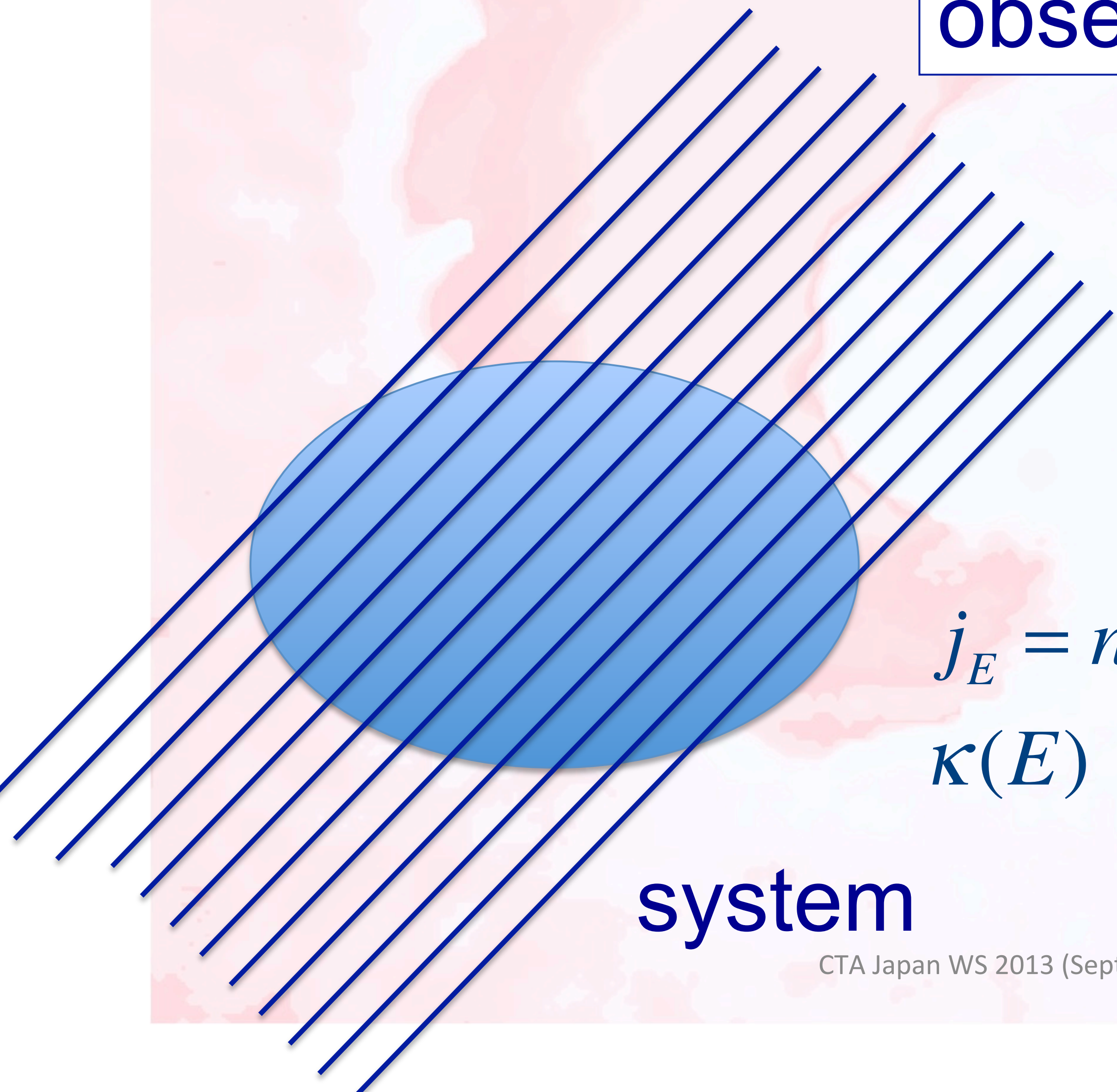

computation of the radiative transfer for a series of 1D rays for every energy E

$$j_E = n_e n_i \Lambda(E,T)$$

$$\kappa(E)$$

Stellar, wind, and orbital parameters for LS 5039 accretion simulations

	Primary	Secondary
Spectral Type	O6.5V	pulsar
Mass	22.9Msun	1.4Msun
Radius	9.3Rsun	---
Vinf	2,440 km/s	12,200 km/s
T_{wind}	39,000 K	---
Mdot	2.5×10^{-7}Msun/yr	---
Porb	3.9060 days	
Eccentricity	0.35	

3D structure of the interaction surface

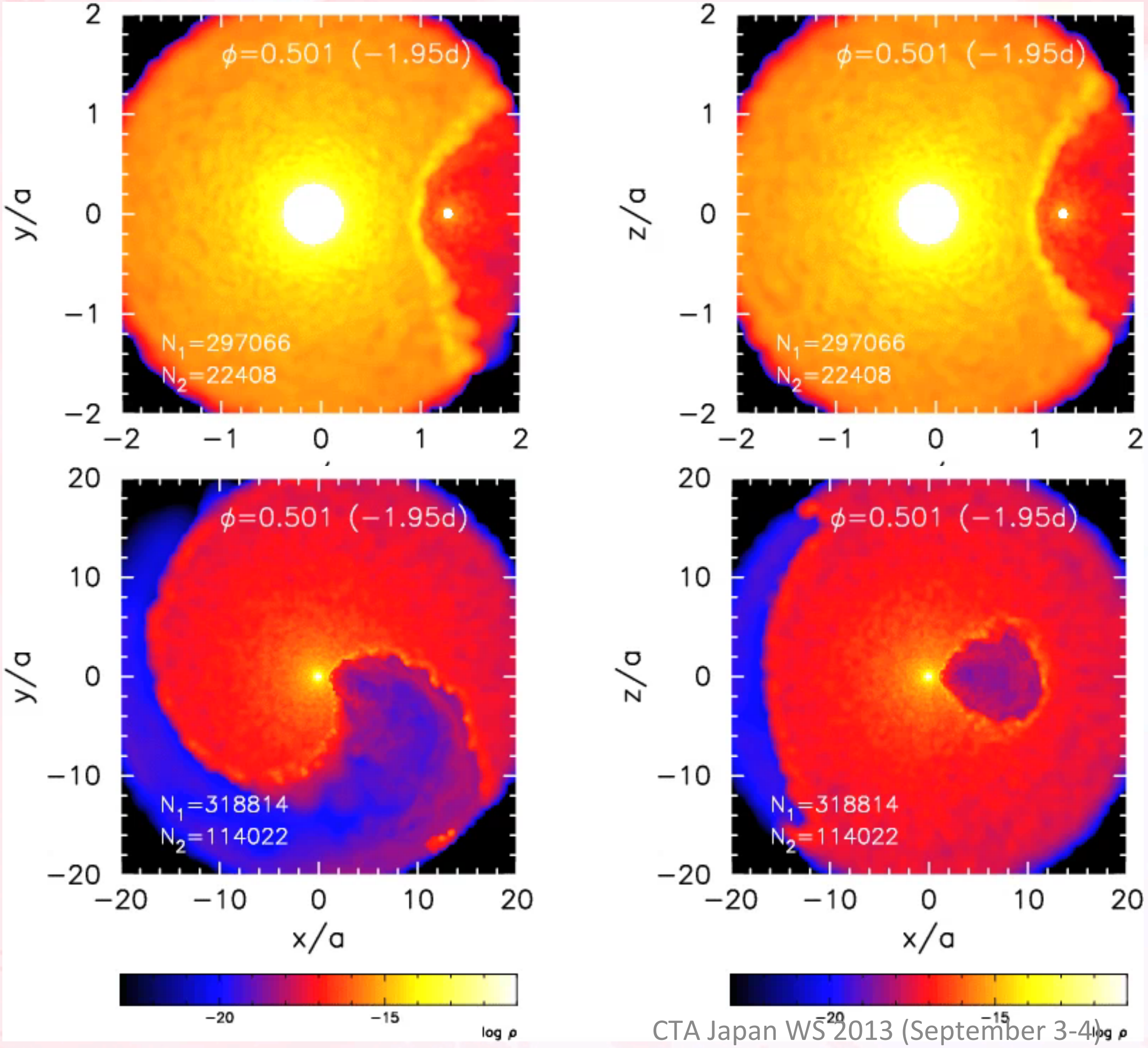

- PW carves out stellar wind.
- PW region has similar dimension in *r* and *z*

$$L_{sd} = 5 \times 10^{36}\,\mathrm{erg/s}$$

large-scale structure of interaction surface

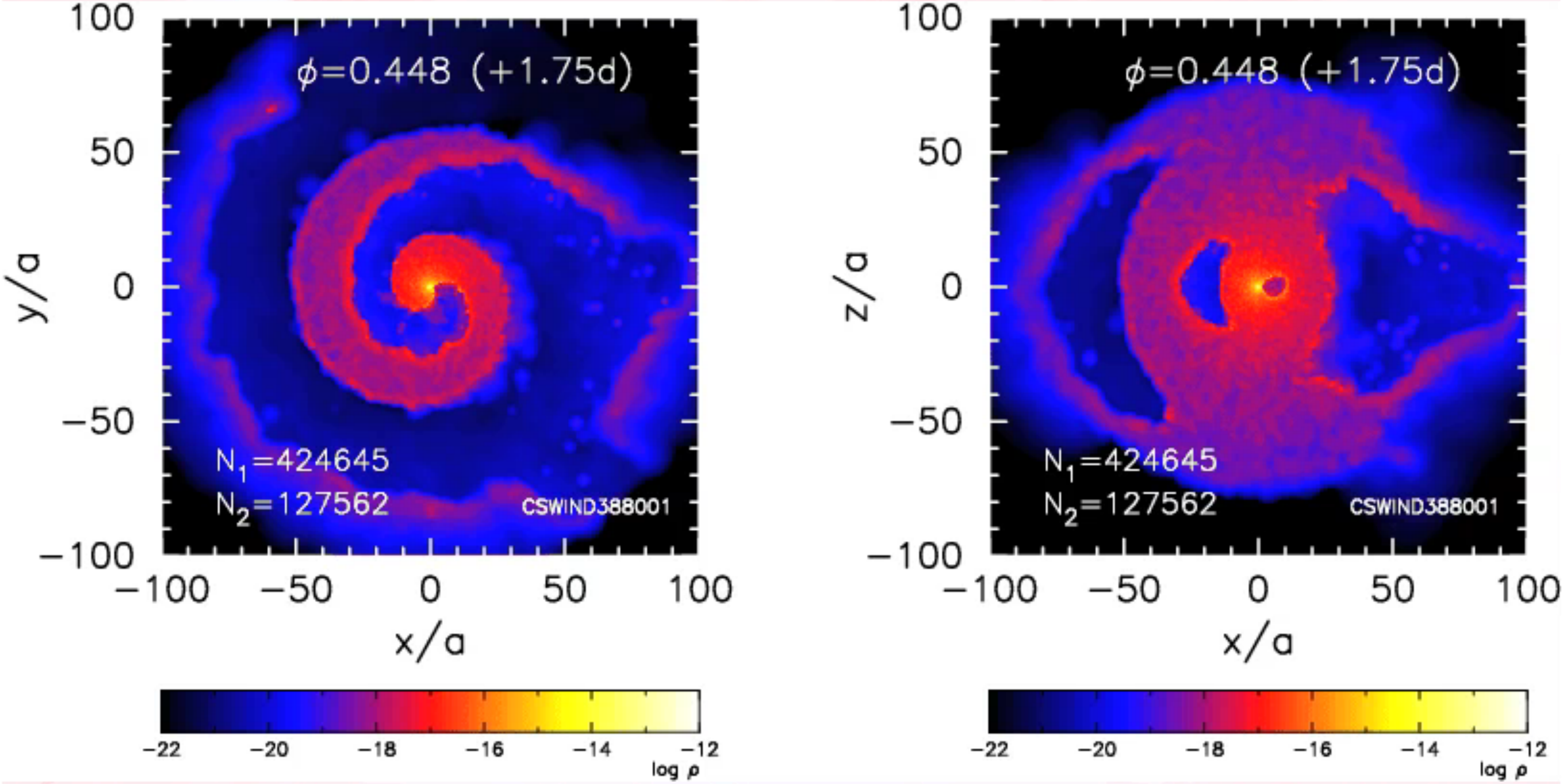

Effect of PW luminosity

$$L_{\rm sd} = 5\times 10^{37}\,{\rm erg/s}$$

$$L_{\rm sd} = 5\times 10^{35}\,{\rm erg/s}$$

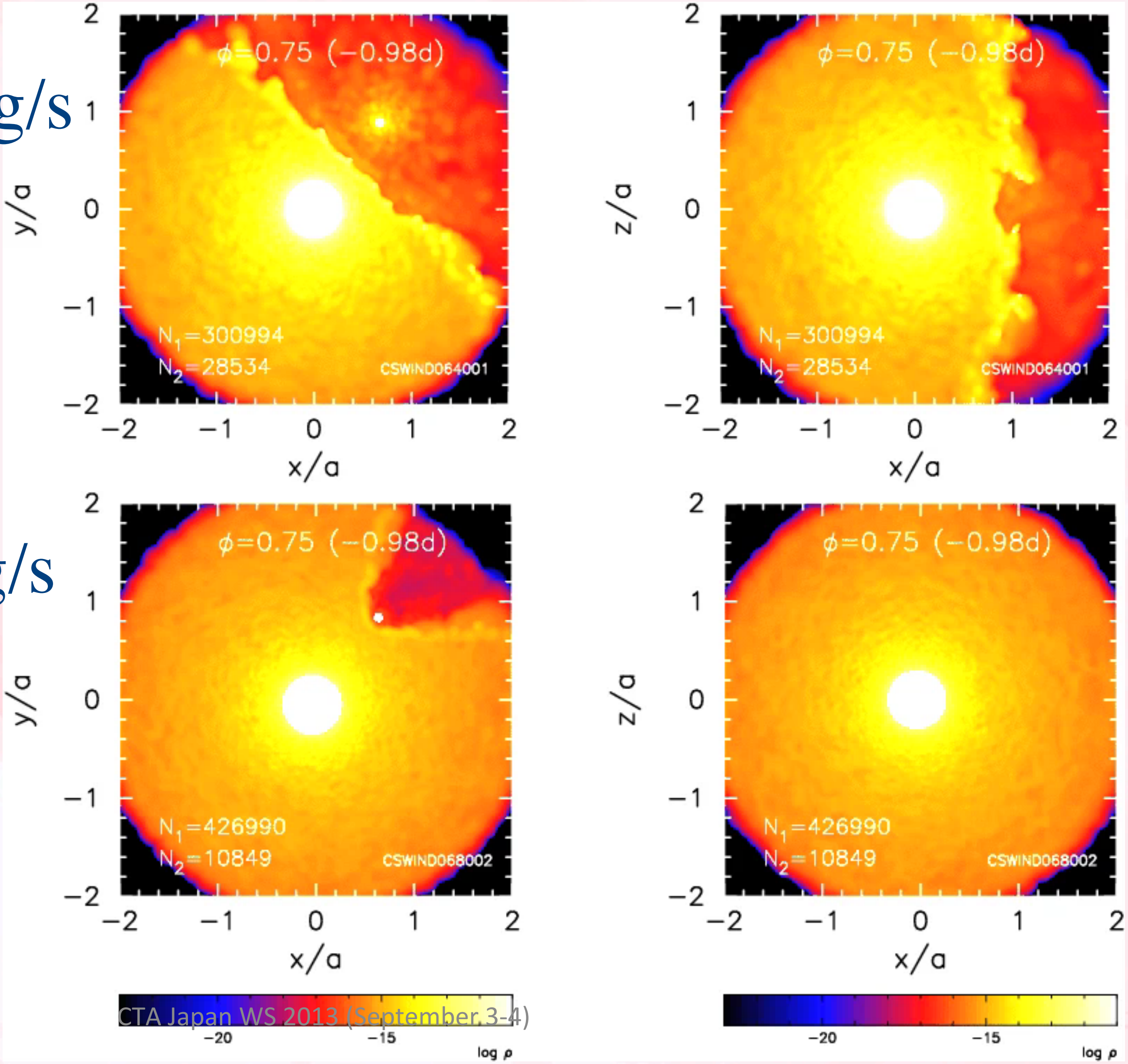

Simulated thermal X-ray spectra

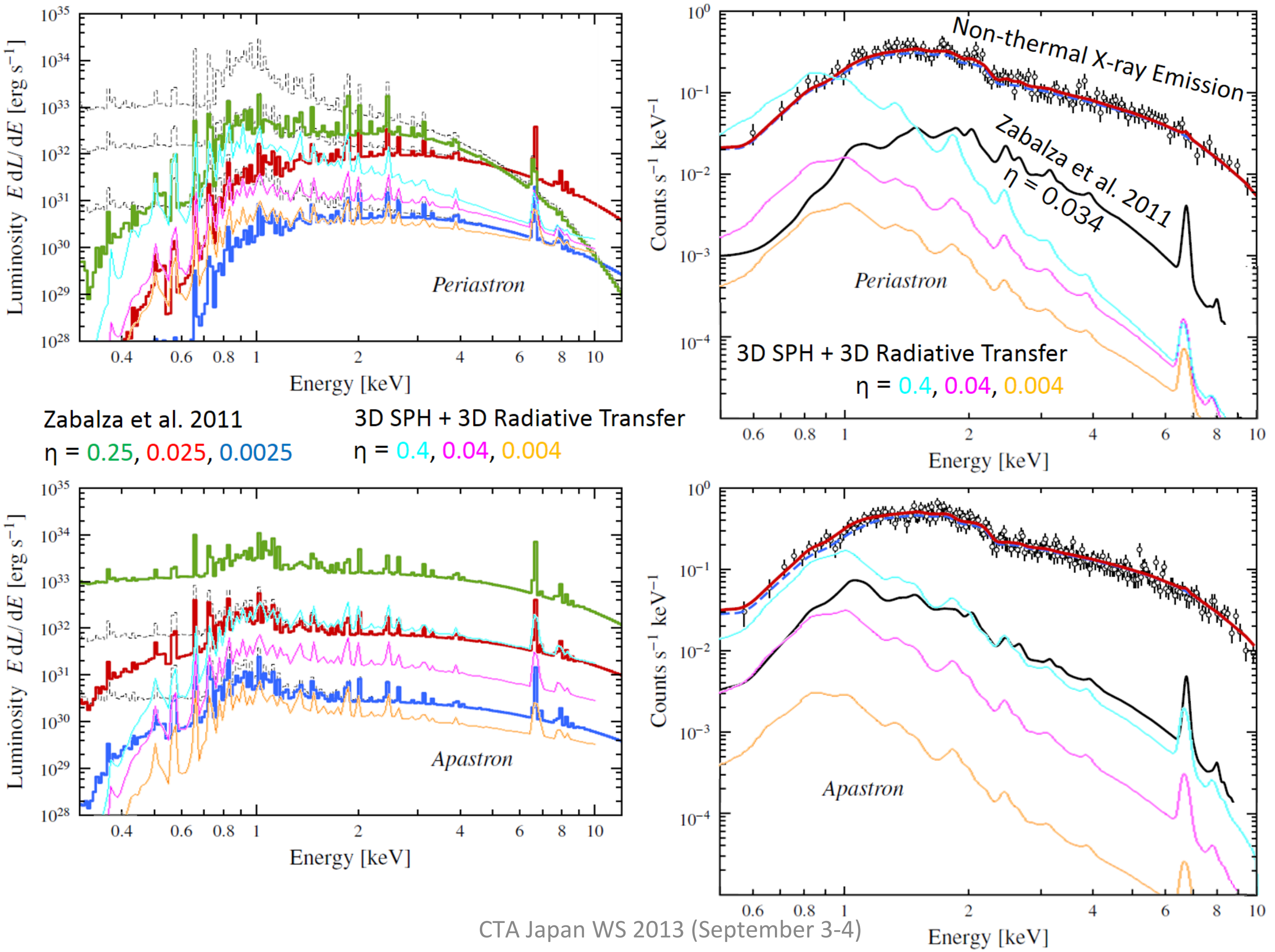

Simulated thermal X-ray light curve

$$L_{sd} = 5 \times 10^{36} \,\mathrm{erg/s}$$

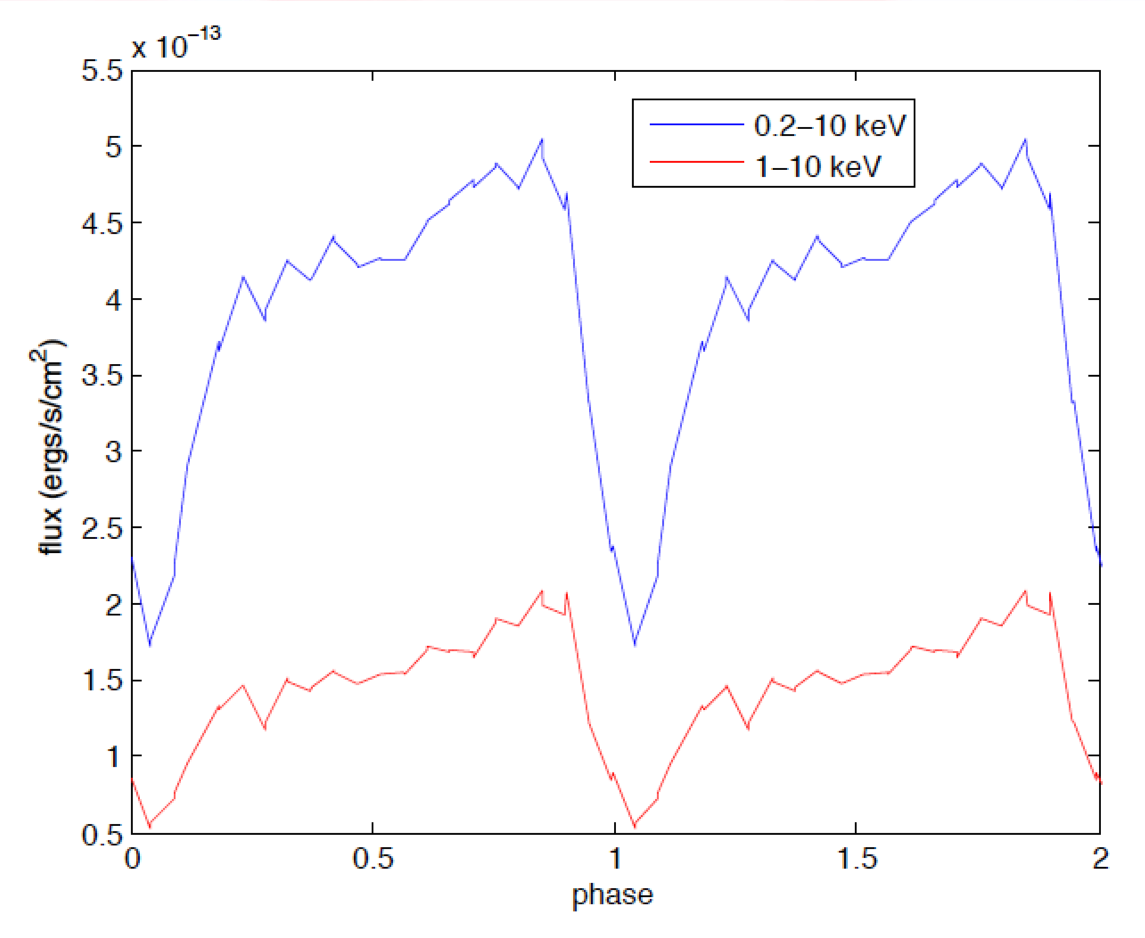

Thermal X-ray flux is higher at INFC than at SUPC because of lower absorption and higher stellar wind velocity at INFC.

Concluding remarks

- Simulated thermal X-ray flux is about one order of magnitude lower than the analytical one.

  ⇨ Higher upper limit of pulsar spin down luminosity by ~10.

- 3D numerical simulations will provide a powerful tool to understand the nature of individual systems and establish a classification/unification scheme of VHE gamma-ray binaries.